Showalter, A.K. (1953): "A stability index for thunderstorm forecasting". *Bulletin of the American Meteorological Society*, **34**, 250–252.
Sutcliffe, R.C. (1947): "A contribution to the problem of development". *Quarterly Journal of the Royal Meteorological Society*, **73**, pp. 370–383.
Tomás-Quevedo, A. (1963): "Meteorological Aspects of the Floods in Catalonia", (in Spanish). *Est. Geograf.*, **91**, 137–146.
Trenberth, K.E. (1978): On the interpretation of the diagnostic quai-geostrophic omega equation. *Monthly Weather Review*, **106**, pp. 131–137.
Unden, P. (1982): "The Swedish Limited Area Model". *SMHI Reports*, Meteorology and Climatology. RMK-35.
Weisman, M.L. and Klemp, J.B. (1982): "The dependence of numerically simulated convective storms on vertical wind shear and bouyancy". *Monthly Weather Review*. **110**, 504–520.

Remote Sensing Reviews, 1996, Vol. 14, pp. 91–117
Reprints available directly from the publisher
Photocopying permitted by license only

Multisensor Observations during the Flood Event of 4–6 November, 1994 over Northern Italy

GIORGIO BONI[a], MAURIZIO CONTI[a], STEFANO DIETRICH[b], LUCA LANZA[a], FRANK S. MARZANO[c], ALBERTO MUGNAI[b], GIULIA PANEGROSSI[b,d] and FRANCO SICCARDI[a]

[a]*Institute of Hydraulics, University of Genova, Montallegro 1, 16145 Genova, Italy;* [b]*Istituto di Fisica dell'Atmosfera - Consiglio Nazionale delle Ricerche (CNR), Via Galilei, 00044 Frascati, Rome, Italy;* [c]*Dipartimento di Ingegneria Elettronica, Universita' "La Sapienza", Eudossiana 18, 00184 Rome, Italy;* [d]*Fondazione per la Meteorologia Applicata, Piazzale delle Cascine 18, 50144 Fierenze, Italy*

(Received 13 April 1995; Revised 25 September 1995; In final form 14 March 1996)

In the perspective of flood hazard multisensor monitoring, the event of 4–6 November, 1994 over Northern Italy is described and analyzed in this paper using traditional ground-based rainfall observations and remote sensing techniques. Satellite imagery is used with different objectives: the interpretation of SAR measurements allows the identification of flooded areas, Meteosat infrared images show high intensity rain areas and SSM/I passive microwave data provide estimates of the rain-rates. The IFA-SAP algorithm, a profile based retrieval technique for estimating rainfall rates and precipitating cloud parameters from spaceborne multifrequency microwave radiometers, has been used in the latter case. The use of multisensor observations considerably supplements conventional monitoring systems which prove inadequate for many hydrological purposes. The present paper is written in the spirit of encouraging *a posteriori* analyses of observed heavy rainfall events so as to explore the potential of a real-time operational integrated system.

I. INTRODUCTION

The disastrous flooding event observed on 4–6 November, 1994 over northern Italy produced inundations in medium to large size subcatchments of the Po River basin, causing several casualties and damage to the properties in the flooded areas. The event presents some meteorological features typical of the Autumn season in the Mediterranean regions of southern Europe that can lead,

in some cases, to extreme events. Specifically, the synoptic meteorological conditions are characterized by sudden modifications as the summer eastward extension of the Azores high pressure cell collapses. As a result, in Western Europe a pressure fall develops, increasing the probability of heavy convective rainfall in the area. The changes in the synoptic meteorological patterns allow for Atlantic frontal systems to invade those regions and can lead to convective instabilities resulting from thermal effects induced by the relatively high sea surface temperature and from interactions with the orographic chains running close to the coastline (Ramis *et al.* 1995).

The resulting heavy rainfall patterns vary with the structure of the large scale circulation. Two different kinds of general rainfall patterns are observed during the Autumn season. The first one produces large areas of high convective activity, having an extension of the order of a few hundreds of kilometres. These Mesoscale Convective Complexes (MCC) (Maddox, 1980) are generated by the interaction between the mesoscale circulation and local thermal and/or orographic effects and usually move eastward with an average advection velocity of about 10–15 m s^{-1}. In the shadow of such systems, convective cells of a few kilometres in size develop, with a temporal evolution of the order of one hour. Rain-gauge observations at the ground typically show a succession of showers with duration of a few hours and with rainfall depths exceeding in some cases one-third to one-half of the total annual average precipitation at each single site. The space-time rainfall characteristics of such storms are likely to produce flash floods in small size river catchments along the Mediterranean slopes from southern Spain to the Tyrrhenian side of the Apennines.

The second typical synoptic pattern presents quite similar features, except for the presence of a high pressure centre over eastern Europe which reduces the advection velocity of the system. The Meteosat observations in the IR band generally show relatively high values of the cloud top temperatures with respect to those observed in the previous case, not allowing the definition of a MCC in the sense indicated by Maddox (1980). This fact indicates lower convective activity and more diffused stratiform rainfall. In this case the precipitation area remains quite steady, thus enlarging the time window in which the rainfall depths observed by different rain-gauges have high correlation. As a consequence, large flood peaks are observed in medium-to-large size catchments, as in the upper Po River basin. However, individual cells of intense convective activity and higher advection velocity, embedded in the major circulation system, may develop and produce critical situations in smaller basins.

The rainfall pattern of the November 1994 event over northern Italy basically belongs to the second of the above mentioned cases. This paper aims to describe and analyse this precipitation event by using ground-based and space-borne multisensor measurements. In Section II, the ground effects of the storm are

illustrated by showing some Synthetic Aperture Radar (SAR) satellite images. In Section III, a description of the event as observed at the ground is addressed by analyzing a series of rain-gauge data in the Piemonte region. Section IV provides some discussion about the use of the infrared radiometer observations on board geostationary platforms for quantitative rainfall estimation, followed by the description of the meteorological situation as observed by the Meteosat radiometer during the analyzed event. A review of a Special Sensor Microwave/Imager (SSM/I) system and a description of a passive microwave precipitation retrieval algorithm are provided in Section V, together with a discussion of the rainfall rates estimated from SSM/I over the Piemonte region. Finally, a few considerations about the usefulness of *a posteriori* investigation of disastrous flooding events are given in the conclusions.

II. THE FLOODING EVENTS

The first SAR operating at frequency of 1275 GHz to obtain images with ground resolution of 25 × 25 m across a 100 km swath was launched in 1978 on board the Seasat satellite. Unfortunately the Seasat SAR failed a few months after the launch. In the following years, SAR imagery from space continued to grow in importance: Space Shuttle flights carried satellites equipped with SAR and future launches are planned. Since features of the Earth surface stand out in the SAR images, the latter can be useful in several fields of Earth science (e.g. analysis of sea wave characteristics in the open ocean, monitoring of coastal processes, geological and hydrological studies). The usefulness of the SAR imagery in monitoring flooded areas is straightforward. In particular, an overall view of the situation allows an early estimation of the extension of flooded areas and of the overflowed water volumes for a better understanding of the flood dynamics and support for decision makers in organizing aid to the population.

The ground effects of the northern Italy flooding event can be extensively examined by using images provided by the SAR sensor on board the polar-orbiting Earth Renources Satellite 1 (ERS-1). ERS-1 follows a near-polar sun-synchronous orbit at an altitude of 777 km. The repeat cycle ranges from three to 31 days, depending on the mission purposes. The ERS-1 SAR has a vertically-polarized channel at 5.3 GHz with a forward-looking ground resolution of 30 × 30 m, a swath of 100 km, a mean incidence angle of 23 degrees and a radiometric accuracy of 2.5 dB.

Even if the weather conditions were at their worst, the ESA (European Space Agency) ERS-1 satellite was able to acquire images of the flooded area similar to that reported in Figure 1: the dark blue indicates flooded areas, while the light

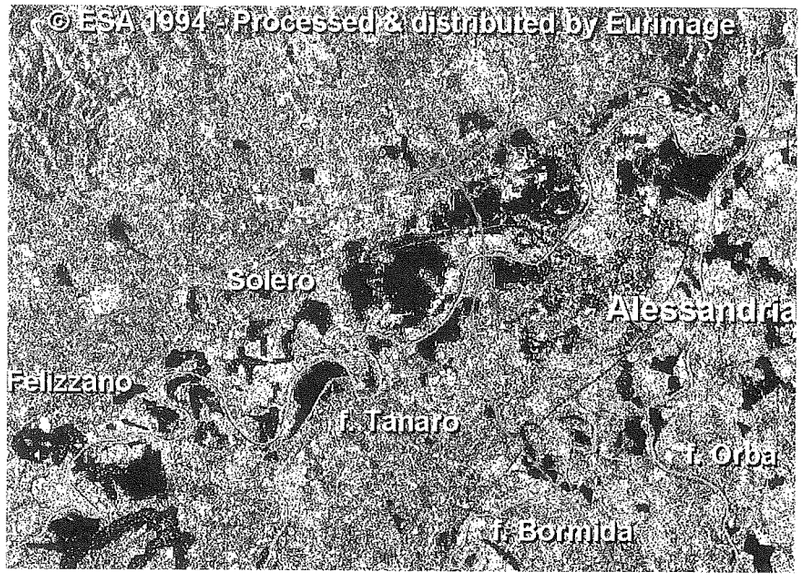

FIGURE 1 Image of the flooded areas observed by SAR (© ESA 1994). (See Colour Plate VIII at the back of the journal).

areas represent cities and small villages. The region of concern is the south-west Piemonte region, near the city of Alessandria, flooded by the Tanaro River. The narrow red strips crossing the image represents highways interrupted by the flood.

The Tanaro River overflowed from the late evening of 5 November to the early morning of 6 November, causing several casualties and considerable damage to property and breakdown of highway and railway bridges, isolating the whole area. The analysis of the SAR image shows quite clearly the extent of the flooded areas reaching the order of several hundred square kilometres (mainly included in a strip of land containing the meanders of the river). Several towns were affected by the flood: the locations of the towns of Felizzano, Solero and of the city of Alessandria are indicated in the image. The Bormida and Orba Rivers, two tributaries of the Tanaro River, overflowed causing further damages near the confluence.

The 30 × 30 m spatial resolution of the SAR is well suited to flood hazard applications, but the large scale of the temporal sampling strongly reduces the suitability of ERS-1 SAR imagery in the framework of operational procedures for real-time flash-flood management. However, the information content of the

imagery can be exploited comparing images surveyed before and after the flooding event for a careful distinction between the flooded areas and those normally covered by water (e.g. rice fields).

III. RAIN-GAUGE OBSERVATIONS

The rainfall field at the ground is described herein by means of daily cumulative rainfall depths as recorded on 4, 5, 6 November by a series of rain-gauges belonging to the "Servizio Idrografico" official network placed along the arc of the Italian Alps in the territory of the Piemonte region. In order to provide an overall view of the evolution of the observed event, point rainfall depth observations were interpolated over the whole region of interest using kriging techniques. In Figure 2, a map indicating the area of interest and its relative position in Italy is indicated. In Figures 3, 4 and 5, the same area is magnified and the isohyets obtained from the spatial interpolation of the rainfall data of the 4, 5 and 6 of November are reported respectively. Note that the Tanaro River basin, where the major floods occurred, is located in the lower part of the area depicted in the Figures.

During 4 November, no rain was observed by a large number of the available gauges. Only a few stations in the northern mountainous part of Piemonte measured values of total rainfall depth around few tens of millimetres (see Figure 3). The next day the precipitation field propagated over the whole area with cumulative depths around 100 mm and areas with daily rain depths exceeding 200 mm (observed maximum 440 mm) localised over the Valle d'Aosta region of northern Italy, probably due to the presence of convective cells embedded in the major circulation pattern (see Figure 4). During 6 November, the intensity of the phenomena lessened in southern Piemonte, where total rainfall depths below 100 mm were observed. Heavy rainfall persisted over northern Piemonte, in the Alpine region; the rain-gauges observed rain depths between 200 and 300 mm, probably caused in part by localised enhanced convective activity in the presence of accentuated orographic chains.

The analysis of ground-based observations shows the steady nature of the phenomena during the second two days, associated with quite light precipitation (average rainfall intensities are estimated around 5–10 mm h^{-1}). This result is in agreement with the fact that rivers draining some medium-to-large size catchments were responsible for the large part of the flooding and damage. The persistent nature of the rainfall pattern is also confirmed by the observations provided by satellite sensors as described in the following sections.

FIGURE 2 Position of the areas concerned by the event of 4–6 November, 1994

IV. METEOSAT OBSERVATIONS

A. The Meteosat Geostationary Satellite

The Meteosat platform belongs to the family of geostationary meteorological satellites, used since the late 1960s for the continuous observation of the atmosphere over specific areas of interest. The technology for geostationary orbiting platforms was developed in order to compensate, in terms of temporal resolu-

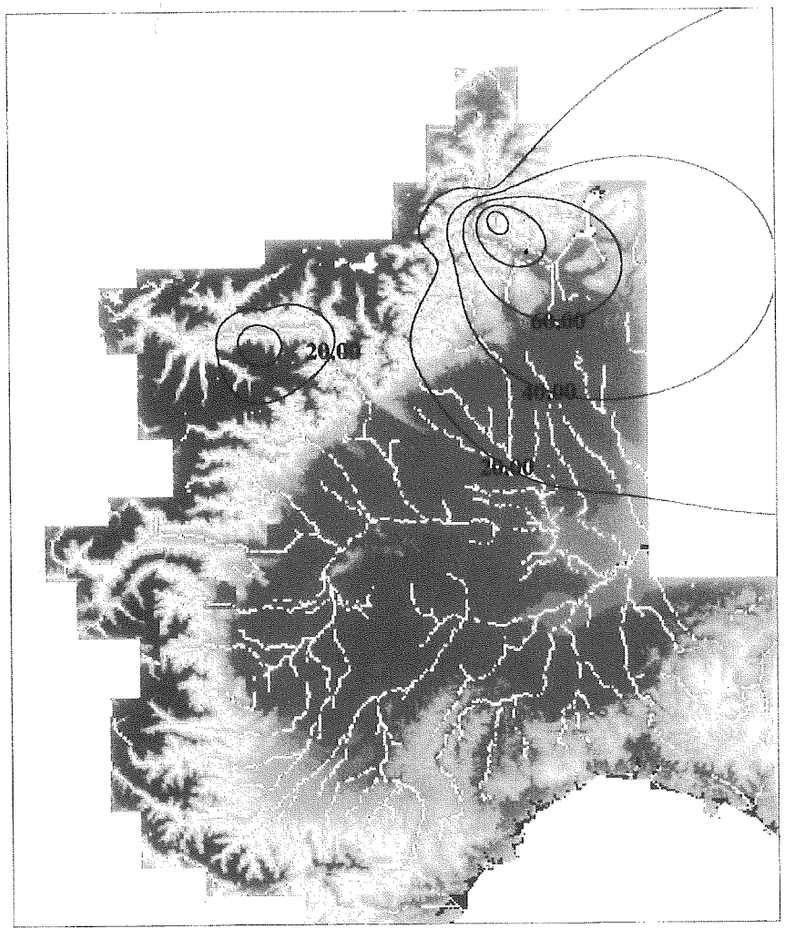

FIGURE 3 Daily cumulative rainfall depth observed by rain-gauges over north-western Italy, 4 November, 1994. (See Colour Plate IX at the back of the journal).

tion, for the infrequent observations of the Earth's surface and atmosphere as provided by polar satellite sensors; these provide scans of the same area only twice a day (or less). In the early 1970s the need for satisfying the requirements of the various European meteorological services and the willingness to collaborate in important programmes of the World Meteorological Organization induced ESA to start the Meteosat programme and realise an European geostation-

November 5th, 1994 - Total rainfall depth [mm]

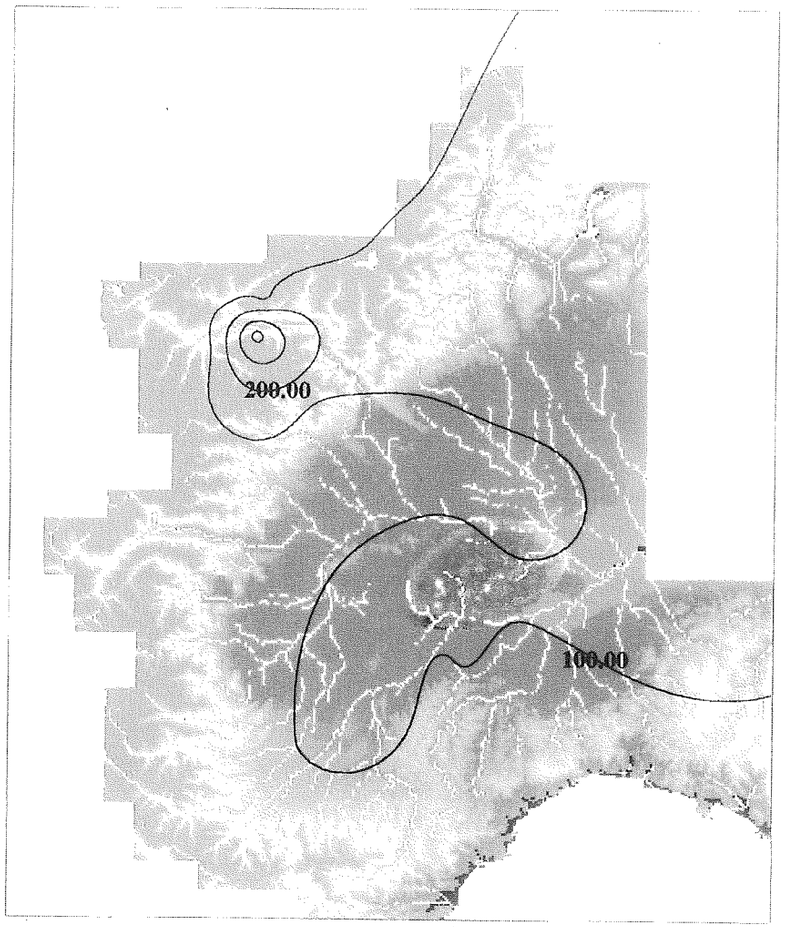

FIGURE 4 Daily cumulative rainfall depth observed by rain-gauges over north-western Italy, 5 November, 1994. (See Colour Plate X at the back of the journal).

ary orbiting platform. Meteosat-1 was launched in 1977 and after a few years of experimental missions the Meteosat Operational Programme (MOP) was started in November 1983; this will continue until the end of 1996.

The Meteosat is presently positioned at 0°N, 0°E and carries the VISSR (Visible and Infrared Spin Scan Radiometer) that provides half hourly images of the whole Earth disc in three different bands: visible (VIS) thermal infrared (IR)

November 6th, 1994 - Total rainfall depth [mm]

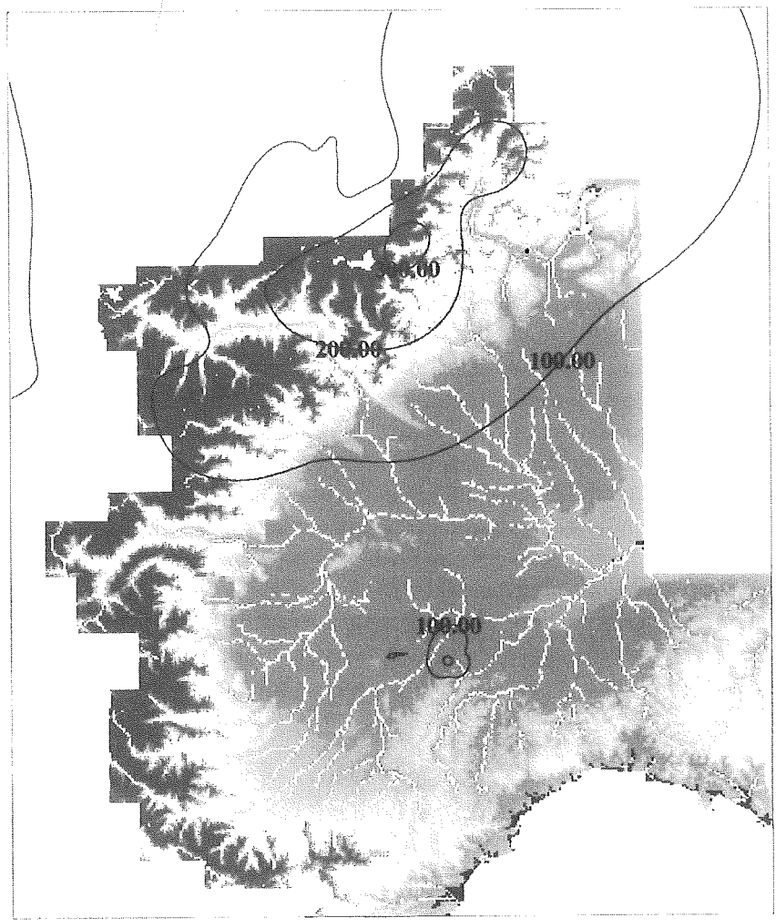

FIGURE 5 Daily cumulative rainfall depth observed by rain-gauges over north-western Italy, 6 November, 1994. (See Colour Plate XI at the back of the journal).

and water vapour absorption band (WV). The VISSR scans the visible Earth disc from east to west and from south to north. The lines of the image are generated by the radiometer during the revolution of the satellite, with a period of 0.6 seconds, and the succession of various lines is obtained by rotating the telescope of the radiometer, synchronized with the revolution period of the satellite, from south to north. The period of acquisition of the images is 25 minutes, followed

by a period of five minutes for the repositioning of the telescope. The images obtained are formed by arrays of 5000 × 5000 (in the VIS band) and 2500 × 2500 (in the IR and WV bands) discrete elements (pixels) respectively that correspond to resolutions of 2.5 × 2.5 km and 5 × 5 km over the Equator. In middle latitudes, due to the Earth's curvature, the resolution degrades to 7 × 5 km in the IR and WV bands.

The images provided by the geostationary satellites have been used for cloud tracking (see Bolla *et al.*, 1995) and for quantitative rainfall estimation (see for example Barrett and Martin (1981) and Atlas and Thiele (1981) for reviews of the various estimation methods) by relying essentially on empirical relationships. Basically, in the VIS band, clouds with highest values of reflectivity have highest rainfall probability and correspondingly, in the IR band, coldest clouds denote more precipitation prone formations. The uncertainty of such estimates is quite large as no information about the inner microphysics of cloud systems is detectable from the images. The estimates of "instantaneous" rainfall at the ground are thus reliable only at the scale of the cloud aggregates. As a result, quantitative estimation of rainfall rates at the ground from IR data is most appropriate when climatological analysis is performed (e.g., when the assessment of monthly to annual precipitation over large regions is concerned for agricultural, climatological or water balance purposes). The use of IR data for "instantaneous" rainfall estimation in flood forecasting is limited to the analysis of the hydrological response of large size catchments. However, IR images can give information about potentially hazardous precipitating systems as highlighted by those regions of the cloud coverage presenting the lowest values of the radiance temperature.

B. Mesoscale Description of the Meteorological Situation Using Meteosat IR Images

The description of the mesoscale meteorological situation producing large floods over northern Italy during November 1994 is performed using a series of Meteosat images in the IR band from 0030 GMT of 4 November to 0500 GMT of 6 November 1994.

At 0030 on 4 November the situation was characterized by a large frontal system extending from the African coast to the British Isles moving slowly east/south-east pushed by a cold airflow drawn from the north by a cyclone positioned west of the British Isles, over the Atlantic Ocean. The advection velocity of the front is strongly limited down by the presence of a strong high pressure centre over the Carpathian area. A warm airflow is advected at the same time

from northern Africa, by the described circulation. The frontal system presents wide areas characterized by quite uniform and relatively high radiance temperatures, characteristic of diffuse stratiform precipitation. Cloudy areas, indicative of strong convective activity—associated with low radiance temperatures—were not observed until 1030 GMT, when the coldest cloud area, fed by the southern warm airflow, developed over the Catalonian coastline. The discrimination between cold convective clouds and cirriform clouds is possible in this case comparing the Meteosat observations with the SSM/I data (see Section V). However, the coldest cloud coverage rapidly exhausted its activity. Around 1200 GMT the combination of the advected flow from northern Africa and the orography of the Liguria region in northern Italy caused some release of instability, generating a storm cell over the city of Genova and the central part of Liguria that caused several failures of the sewer systems and problems on the road system.

At about 1530 GMT new convective clouds developed over south-west France and extended progressively to the entire western part of France. Even this second convective cloud area is characterized by a quite rapid evolution. The continuous contribution of warm air provided by the African airflow generated a third area of convective activity around 2130–2200 GMT of 4 November over the Pyrenees. The area extended rapidly and progressively over south-central and northern France, until the early morning of 5 November. During this period the frontal system, embedding various smaller areas with deep convective activity, displaced very slowly eastwards. Northern Italy was progressively affected by the front since the late morning of the same day. In the afternoon the frontal system reached north-west Italy and the islands of Sardinia and Corsica, thus generating convective activity over these areas. During the night time, the eastern high pressure cell declined and the front was advected by the Atlantic currents toward the Adriatic Sea and central Europe during the morning of 6 November.

Relatively warm precipitating clouds as identified in the sequence of Meteosat images persisted for several hours above the upper Po River basin, starting on the late morning of 5 November and for a large part of the next day while isolated convective cells developed embedded within the front. These observations are confirmed by the ground based measurement described in the previous section (Figures 3, 4 and 5) and a fairly good correspondence is found between the persistence of the observed precipitating clouds over the area of interest and that of the rain during 5 and 6 November.

Aiming at a better understanding of the potential of using sequences of Meteosat images to describe the overall characteristics of different meteorological patterns, the extreme rainfall event which occurred on 27–28 September 1992 over the Liguria region of Italy has been considered for comparison also, since

it presented quite different characteristics. In that case a larger area presenting radiance temperature values above 253°K was observed, allowing the identification of a typical Mesoscale Convective Complex (MCC) (Maddox, 1980) that moved quite rapidly from southern France in a south-easterly direction, driven by the outline of the orography that runs almost parallel to the Tyrrhenian coastline of Italy, while the entire cloud system was moving slowly eastwards. In Figure 6, the total areal coverage of the MCC for Liguria event is shown from 0130 GMT of 27 September to 2230 GMT of 28 September 1992. Colour levels represent classes of persistence of the cloud coverage over each pixel.

The event of November 1994 presents quite different characteristics because of the presence of a stable high pressure centre over the Carpathian area, reducing the eastward advection of the frontal system. The sequence of Meteosat images shows that the clouds corresponding to the maximum probability of precipitation were quite persistent over the area investigated but the coldest cloud coverage evolved quite rapidly (low persistence). Figure 7 shows the area covered by clouds with top temperatures above 253°K (namely the part of the cloud system where convection mainly develops) during the whole event. The zones corresponding to the Piemonte region, where major floods occurred, do not present a very high degree of persistence in time since the rainfall was stratiform.

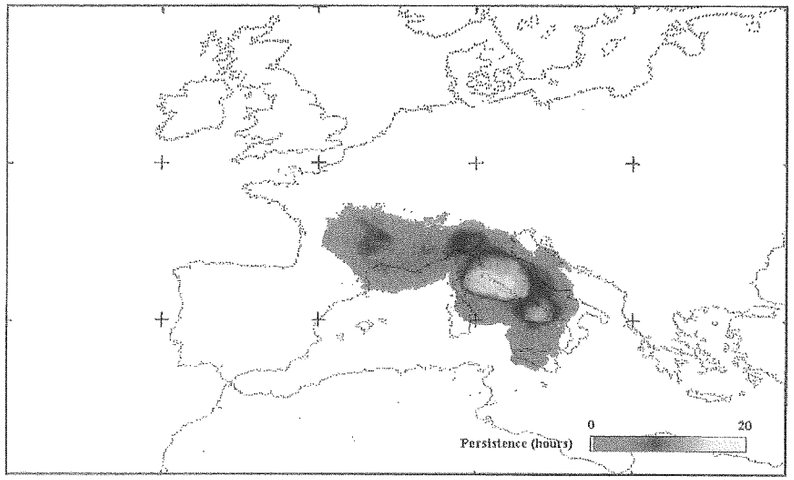

FIGURE 6 Total areal coverage of the MCC for the event of 1992 from 0130 GMT of 27 September to 2230 GMT of 28 September. (See Colour Plate XII at the back of the journal).

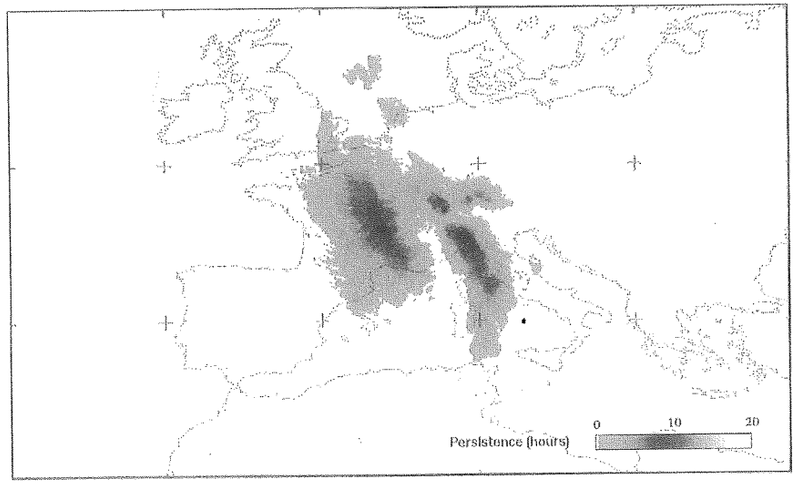

FIGURE 7 Total areal coverage of the coldest clouds for the event of 1994 from 0030 GMT of 5 November to 0500 GMT of 6 November. (See Colour Plate XIII at the back of the journal).

River catchments of different areas produced floods when affected by the two meteorological events with the characteristics described. High intensity rainfall, even of short duration, as occurred in the 1992 Liguria event, are able to produce floods in small size catchments (10–100 km^2), while the persistence in time of precipitation, even if not very intense, affects medium to large size catchments (1000 km^2 and more) in the Piemonte 1994 event. From the point of view of the Meteosat images, the first kind of events is characterised by short persistence, but quite low values of radiance temperatures (intense rainfall); on the contrary, the second kind of event is characterised by long persistence and higher values of radiance temperatures (light rainfall). Figures 8 and 9 show the persistence of the entire cloud systems with embedding convective clouds for the two case studies. Yellow to red areas are associated with the highest persistence values, i.e. higher values of rainfall depth.

Comparing the persistence in time of the convective clouds with the cumulative values of the persistence of the cloud systems as a whole, the features of the events described above are easily distinguishable (Boni *et al.* 1995). In September 1992 floods occurred over small size catchments in the Liguria region of Italy, and the images shows relatively short persistence (see Figure 8) and very low values of the radiance temperature associated with the MCC (see Figure 6). On the contrary during the second event, which produced floods over large size catchments in northern Italy, higher persistence and higher values of the radiance temperature are observed (see Figures 9 and 7 respectively).

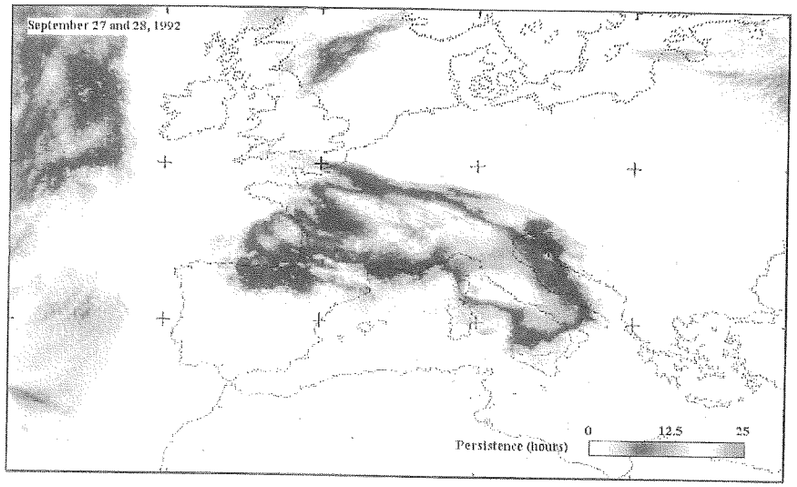

FIGURE 8 Total areal coverage of the cloud system for the event of 1992 from 0130 GMT of 27 September to 2230 GMT of 28 September. (See Colour Plate XIV at the back of the journal).

V. SSM/I OBSERVATIONS AND RESULTS

A. SSM/I System Description

Because of its characteristics, the Special Sensor Microwave/Imager (SSM/I) on board spacecraft of the US Defense Meteorological Satellite Program (DMSP) was a major breakthrough (Spencer *et al.* 1989) for rainfall monitoring from space. The SSM/I can provide information on a variety of environmental parameters, including atmospheric water, wind speed, and sea ice (Hollinger *et al.* 1990). It is a seven-channel, four-frequency (19.35, 22.235, 37.0, and 85.5 GHz) conically-scanning passive-microwave radiometer system, operating in dual polarization (both vertical and horizontal) at each frequency except 22 GHz where only vertical polarization is measured: this channel corresponds to a water vapour absorption line and is primarily used to monitor atmospheric water vapour to correct for atmospheric attenuation. Each DMSP satellite flies in a circular sun-synchronous near-polar orbit at an altitude of about 850 km, with a period of 102 minutes for a total of 14.1 orbits per day. For the F8 spacecraft, the equatorial ascending node is at 0613 local time, while for the F11 it is at 1704 local time. Data are collected during 102° of this rotation (±51° about the aft direction for the F8, and ±51° about the fore direction for the F11) resulting in a swath of about 1400 km. The effective ground resolutions (i.e., the sizes of the antennae footprints on the ground) are about 69 × 43, 60 × 40, 37 × 28, and 15

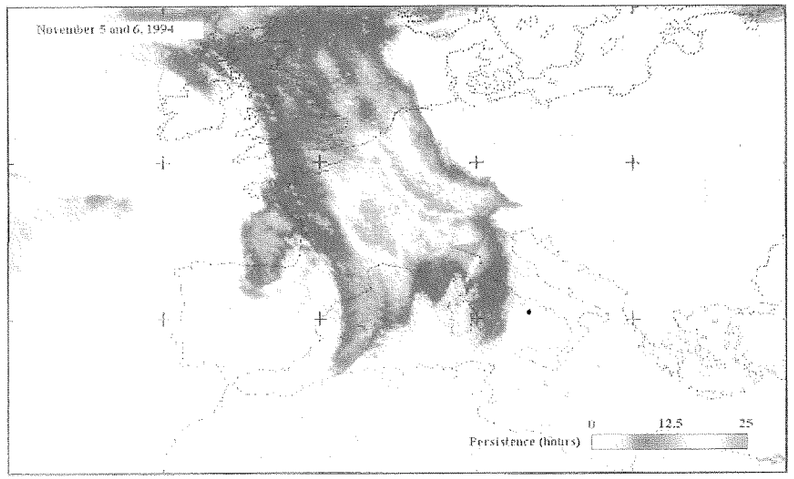

FIGURE 9 Total areal coverage of the cloud system for the event of 1994 from 0030 GMT of 5 November to 0500 GMT of 6 November. (See Colour Plate XV at the back of the journal).

× 13 km at 19, 22, 37, and 85 GHz, respectively (for each frequency, the first value is in the along-track direction, whereas the second value is in the cross-track direction).

It is important to notice two things. First, with the exception of small circular sections at the North and South Poles, which are never measured due to the orbit inclination, many locations on the Earth are observed by the SSM/I up to twice a day (in the early morning in ascending mode, and in the early evening in descending mode); however, due to the limited swath width, the SSM/I Earth coverage in a 24 hour period shows diamond-shaped regions which are not observed, but will be covered within 72 hours. Of course, all this poses serious limitations to the potential of SSM/I measurements for operational flood hazard forecasting. However, this problem would be definitely alleviated by resorting to a network of space-based microwave radiometers (at present, there are two SSM/Is flying aboard DMSP satellites on different orbits) used in conjunction with geostationary satellites operating in the visible/infrared portions of the electromagnetic spectrum. Second, because of the large antenna footprints there is substantial overlap between adjacent measurements for all but the 85 GHz channels, leading to the possibility of retrieving information (deconvolved brightness temperatures), on scales smaller than those directly sensed by the SSM/I antennae (see, for instance, Farrar and Smith, 1992).

B. SSM/I Precipitation Retrieval Algorithm

A precipitation retrieval algorithm based on data from the SSM/I space-borne multi-frequency microwave radiometers, has been developed in Italy within the "Flood hazard multisensor monitoring" CEE programme. Since the algorithm was developed at the *Istituto di Fisica dell'Atmosfera of Consiglio Nazionale delle Ricerche* in Frascati and at the *Dipartimento di Ingegneria Elettronica* of *Università "La Sapienza"* in Roma, it is referred to as the IFA-SAP algorithm. It is based on theoretical studies by Mugnai *et al.* (1990, 1992, 1993, 1994), Smith *et al.* (1992), and Basili *et al.* (1992a, 1992b, 1994) and has been described in detail by Marzano *et al.* (1994, 1995). (See also Smith *et al.*, 1994).

The IFA-SAP algorithm is a profile-based retrieval technique that attempts to tackle some of the possible weaknesses within current microwave algorithms of the same kind, while retaining their basic strengths (Smith *et al.*, 1994; Wilheit *et al.*, 1994). The algorithm is based on a maximum-likelihood discriminant analysis making use of a vast physically-based, statistically-generated, classified cloud-radiation database. At present, the outputs of a three-dimensional time-dependent mesoscale/cloud model (Tripoli, 1992) are utilized as the primary cloud dataset, even though radar products may also be used. For the present work a cloud model simulation of a warm-based cold rain continental storm specifying the expected boundary conditions of the observed event for radiative transfer calculations (e.g. surface emissivity) was chosen. The cloud-radiation database is generated by first applying a multivariate random method, taking into account the correlations among the various cloud profile parameters, and then a plane-parallel radiative transfer scheme to the primary cloud dataset. Given a multi-frequency brightness temperature measurement, the retrieval algorithm uses a maximum-likelihood multivariate criterion to select the most probable cloud structure within the cloud-radiation database—i.e., the cloud structure that minimizes the sum of the Euclidean distance between the multi-frequency simulated and measured T_Bs and of the Bayesian distance between the simulated hydrometeor profiles and their class averages. Thus, from a theoretical point of view, the algorithm uses the cloud-radiation model to obtain an *a priori* knowledge about the vertical structure of the observed precipitating clouds, so as to reduce the inherent ill-conditioning and non-uniqueness of the inverse process. The algorithm is computationally efficient and has been numerically tested. The precipitation retrieval is performed on a pixel by pixel basis, after discriminating the precipitating area by direct tests involving the measured upwelling polarized T_Bs.

The algorithm consists of two phases. During the first phase, a cloud-radiation database is generated so as to define the modeling framework for inversion (*modeling phase*). The second phase is divided into processing of the brightness temperatures measured from space and precipitation estimation (*retrieval phase*). Within the modeling phase (*direct problem*), the aim is to statistically produce a cloud-radiation database which contains a large number (thousands) of cloud structures described by the vertical distribution of various hydrometeors and the related upward brightness temperatures (T_Bs) as observed by a spaceborne or airborne radiometer. The retrieval phase (*inverse problem*) represents the retrieval procedure and implies the processing of measured radiometric data and the estimation of the relevant cloud and precipitation parameters from SSM/I measurements. In particular, the surface rain-rate is derived from a rainfall model based on the estimated vertical profiles of the hydrometeor contents. The main features of the IFA-SAP algorithm can be summarized as follows:

(a) As with any profile-based algorithm, it is most suitable for retrieving instantaneous precipitation, rather than climatological precipitation; thus, it is most appropriate for flash flood monitoring.
(b) As one of such algorithms, it is adapted to the reality that surface rain-rate is only indirectly related to the upwelling microwave radiation at the top of the atmosphere; rain-rates are physically derived through a fallout equation that utilizes the vertical profiles of liquid and ice water contents—which are the fundamental retrieval variables of the algorithm.
(c) As compared with other profile-based algorithms using a perturbation approach during the retrieval phase, it exhibits very good performance in terms of processing time since the algorithm itself is not iterative and the time consuming task of solving the radiative transfer equation is accomplished only once, when generating the cloud-radiation database.
(d) In addition, the use of maximum-likelihood discriminant analysis provides quantitative information on the uncertainty variance associated with a given retrieval—a result which is generally not yielded by profile-based algorithms.
(e) It is based on a physical scheme; therefore, it is flexible to improvements in the embedded physical and numerical techniques. The underlying cloud microphysics are relatively complete because of the use of an explicit cloud/mesoscale model that can be configured to specific environments through appropriately defined simulations.

The IFA-SAP algorithm is being tested during 1995 within two international projects, in which several techniques for retrieving instantaneous rainfall at the pixel scale will be intercompared and validated for a series of heavy precipitation events all over the world, observed by the Special Sensor Microwave/

Imager (SSM/I) radiometers presently flown on board spacecraft of the US DMSP (Hollinger *et al.*, 1990). The first international project is the second phase of the Precipitation Intercomparison Project (PIP-2) of the WetNet Project of the National Aeronautics and Space Administration (NASA) (Dodge and Goodman, 1994); the second project is the Third Algorithm Intercomparison Project (AIP-3) of the Global Precipitation Climatology Project (WMO, 1989).

C. SSM/I Observations of Piemonte Flood Event

As an example of the application of the IFA-SAP retrieval algorithm, we illustrate the results obtained by using SSM/I data of the intense flash-flood event which occurred in Piemonte, Italy on 4–5 November, 1994, previously described.

Figures 10, 11 and 12 show the T_Bs measured by the SSM/I vertical-polarization channel at 85.5 GHz on 4 November at 0544 GMT, on 4 November at 1712 GMT and on 5 November at 1556 GMT, respectively. The attention is focused on the large and widespread cloud system over the north-western part of France on the afternoon of 4 November that reached the north-western part of

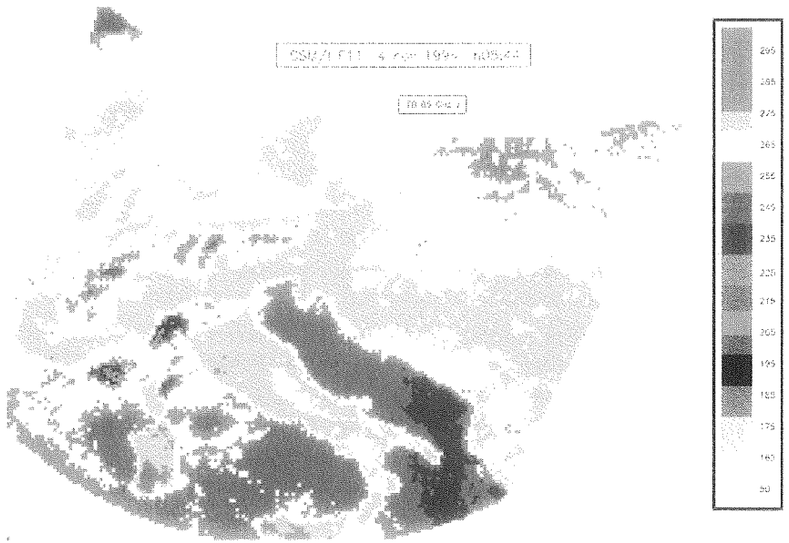

FIGURE 10 Brightness temperatures (T_Bs) measured by the SSM/I vertical-polarization channel at 85.5 GHz on 4 November at 0544 GMT. (See Colour Plate XVI at the back of the journal).

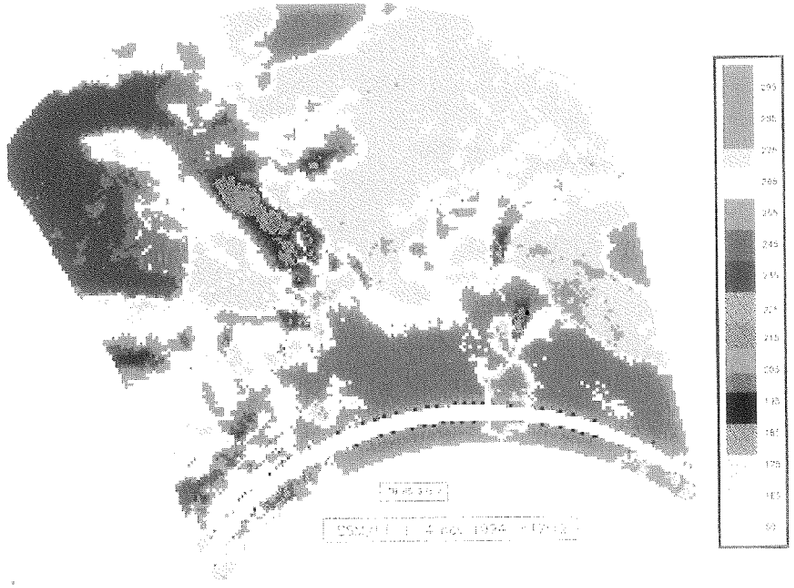

FIGURE 11 Brightness temperatures (T_Bs) measured by the SSM/I vertical-polarization channel at 85.5 GHz, on 4 November at 1712 GMT. (See Colour Plate XVII at the back of the journal).

Italy on 5 November (see Section IV for the description of the evolution of the system from Meteosat imagery). The values of the brightness temperatures associated with the various colours are given in the false-colour palette.

In order to physically interpret the features of the SSM/I image, we have to remember that generally speaking, backscattering from large drops and ice particles is the physical mechanism responsible for the fact that the entire storm system appears as a cool feature over a warm continental background; and the emission of large drops causes rainfall to appear as a warm feature over a cool sea background. Thus, in each image, the grey-to-brown pixels represent the most intense cells within the storms in which large ice particles (which eventually fall and melt to form precipitation drops) are inhibiting the upwelling radiation emitted both from the surface and from the lower rain layers from reaching the satellite radiometer. Surrounding green pixels may indicate light precipitation, while yellow pixels represent non-precipitating clouds and/or high level cirrus clouds. Finally, cloud-free areas are indicated by orange-to-red over land and by green over sea.

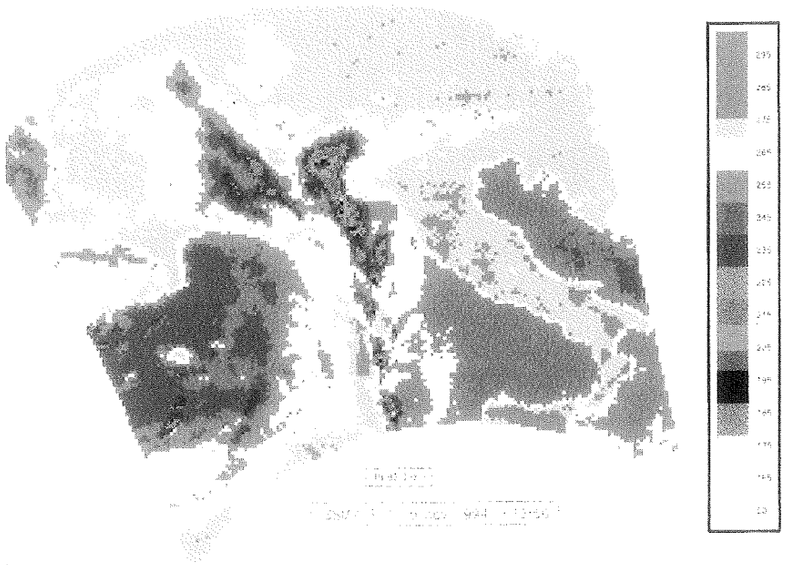

FIGURE 12 Brightness temperatures (T_B) measured by the SSM/I vertical-polarization channel at 85.5 GHz on 5 November at 1556 GMT. (See Colour Plate XVIII at the back of the journal).

The rainfall pattern of Figure 10 is associated with the large frontal system extending from the African coast to the British Isles, producing stratiform precipitation (see Section IV.B). Figure 11 shows the SSM/I detection of the new convective system developed over South-Western France that rapidly extended to the whole of western France on evening of 4 November. Finally, Figure 12 shows that the coldest cloud coverage has already reached northern Italy and the islands of Sardinia and Corsica, generating slight convective rainfall embedded in the frontal system (see Figure 7 for comparison with Meteosat images).

As observed in the previous paragraphs the data provided by the SSM/I allow an easy recognition of the precipitating clouds, in good agreement with the Meteosat and traditional ground based observations. In particular, the agreement with Meteosat data is useful for the discrimination between high thin clouds (e.g. cirri), non-precipitating, and convective clouds, not possible using only the second set of data.

D. SSM/I Rainfall Estimates for Piemonte Flood Event

Figures 13, 14, 15 show the rainfall rate images derived from SSM/I data by means of the IFA-SAP algorithm for the precipitation areas of Figures 10, 11,

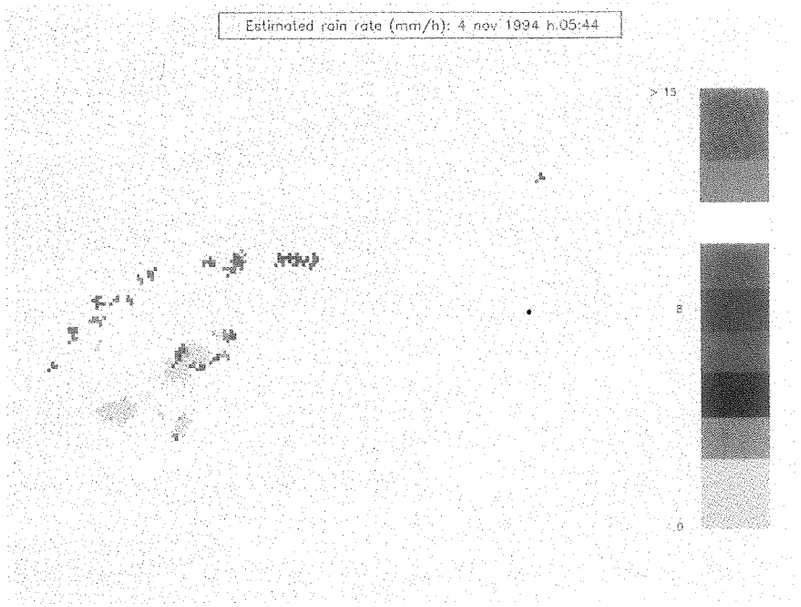

FIGURE 13 Rainfall rate image derived from SSM/I data by means of the IFA-SAP algorithm for the precipitation areas of Figure 10. (See Colour Plate XIX at the back of the journal).

and 12 respectively. The values of the rainfall rates associated with the various colours are given in the false-colour palette. The precipitation areas have been discriminated using an optimized combination of the Polarization Corrected Temperature technique (Spencer *et al.*, 1989) and the Scattering Index technique (Grody, 1991). As expected, the higher rain-rate areas are associated with the north-western part of France on 4 November at 1712 GMT and with the north-western part of Italy on 5 November at 1556 GMT. Heavy convective cells are also present over the Tyrrhenian sea in Figure 15. As expected, the rainfall structures are associated with regions of fairly low values of SSM/I 85 GHz T_Bs.

The comparison between rain-gauge measurements and SSM/I derived rainfall rates is always difficult because of different space-time integration scales. In fact, while the rain-gauges provide point measurements integrated over tens of minutes, the SSM/I can give instantaneous rain-rates over an area of 200 km^2. Thus, in order to avoid these problems, comparisons of statistical distributions of rain-rates over a given region can be used. Figures 16, 17, 18 show the rainfall rate histograms derived from SSM/I data for the precipitation areas over land of Figures 13, 14, and 15, respectively. The minimum detectable rain-rate has been put at 2 mm h^{-1}, a value comparable with the expected retrieval accu-

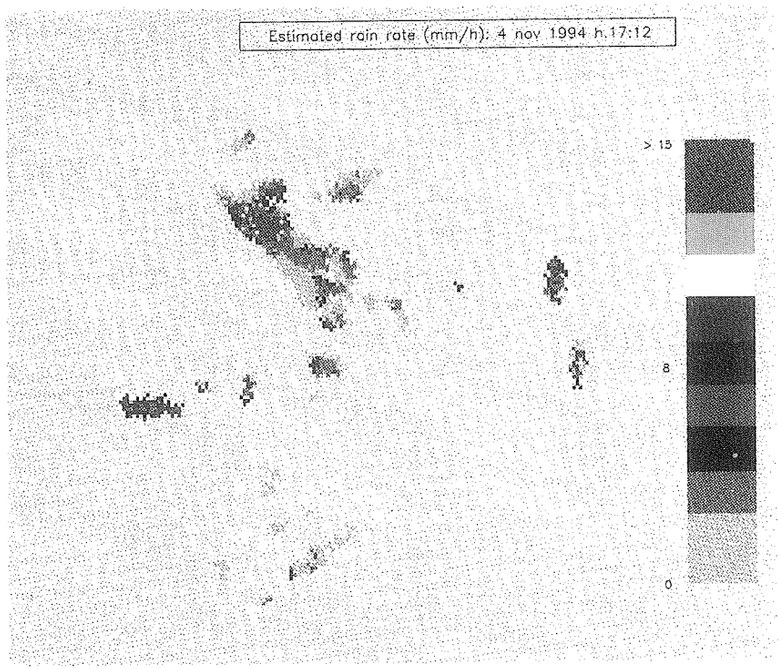

FIGURE 14 Rainfall rate images derived from SSM/I data by means of the IFA-SAP algorithm for the precipitation areas of Figure 11. (See Colour Plate XX at the back of the journal).

racy at lower rain-rates. In all the histograms the ranges of rainfall rates over land goes from few mm h^{-1} to about 20 mm h^{-1} (while the higher values up to 40 mm h^{-1} are associated with the convective rain areas over the sea). In particular, Figure 16 shows a bimodal behaviour of the histogram (due to two different cells), while Figure 18 shows a negative-exponential behaviour. The low values of rain-rates over land as obtained from the IFA-SAP model agree with the observed rainfall depth reported in Section III, derived by rain-gauge measurements. This confirms once again that the meteorological conditions of the analyzed event were dominantly characterized by stratiform rainfall.

VI. CONCLUSIONS

The large flood event which occurred during November 1994 over north-western Italy, producing several casualties and a few thousand of billion Lira of damage

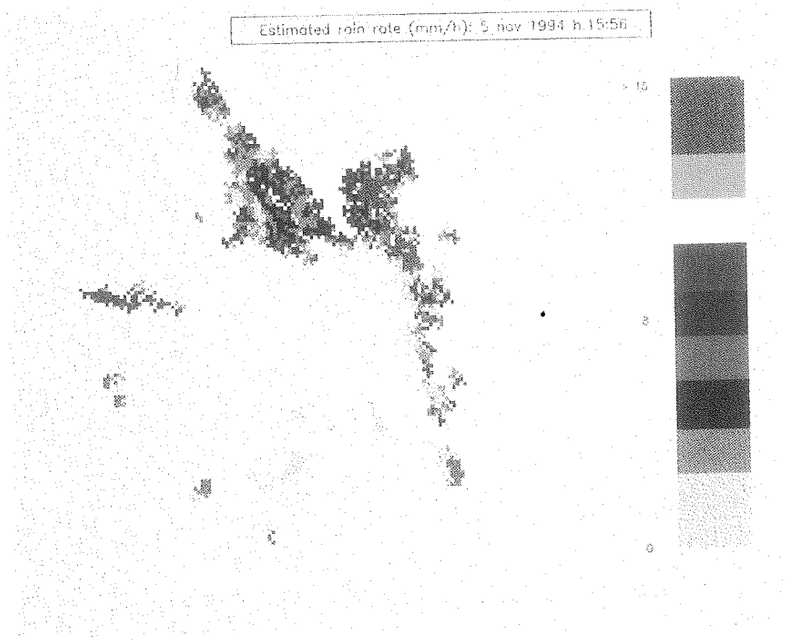

FIGURE 15 Rainfall rate images derived from SSM/I data by means of the IFA-SAP algorithm for the precipitation areas of Figure 12. (See Colour Plate XXI at the back of the journal).

has been described in this paper using multisensor observations. The analysis of satellite data from ERS-1 SAR, Meteosat and SSM/I has been addressed in order to mitigate the inadequacy of the conventional data supplies. The use of Meteosat qualitative analyses of the persistence and intensity of the convective activity over a particular area, and the SSM/I quantitative rainfall estimation, have been presented and compared with the available rain-gauge measurements.

Quantitative comparison with rain-gauge measurements proves quite difficult because of the different spatial and temporal scales of integration with respect to both Meteosat and SSM/I observations. The point observations provided by rain-gauges can be overcome using remotely sensed spatially distributed data like SSM/I and Meteosat observation. The integration of these two sources of data starts from an "initialisation" of the IR cloud top analysis of rainfall using the microwave inversion algorithm that can also provide an estimation of the vertical structure of the cloud. In particular, the SSM/I rainfall estimates can be used

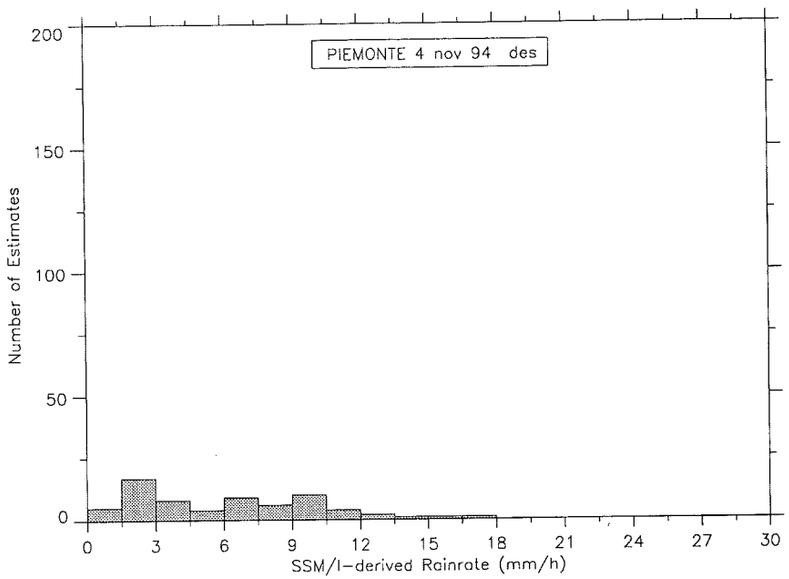

FIGURE 16 Rainfall rate histograms derived from SSM/I data for the precipitation areas over land of Figure 13.

to calibrate the Meteosat cloud cover images in terms of expected surface rainrates. Then the calibrated precipitation areas can be followed in their evolution by looking at the Meteosat image sequence till the cloud system dissipates.

This strategy of combining the use of the SSM/I and Meteosat derived information needs a large rainfall image dataset from both sources to be proved and refined. The *a posteriori* analysis methodology as proposed in this paper can provide a useful background for the identification of the pattern of future events using the information provided by all the available data sources, in the framework of real-time procedures.

The whole set of remotely sensed data can also be exploited for coupling with physically based precipitation forecasting models. The assessment of the initial and boundary conditions of simplified cloud models as developed in recent years (see, for example, French and Krajewski, 1994) can be addressed within the framework of an operational flash-flood forecasting procedure, in order to increase the reliability of river flow predictions for the catchments of concern.

The integration of conventional and remote sensing data for rainfall monitoring and forecasting is indeed expected to produce operational techniques for supporting decision makers during critical meteorological conditions. However, as pointed out by La Barbera and Lanza (1995), a certain degree of caution

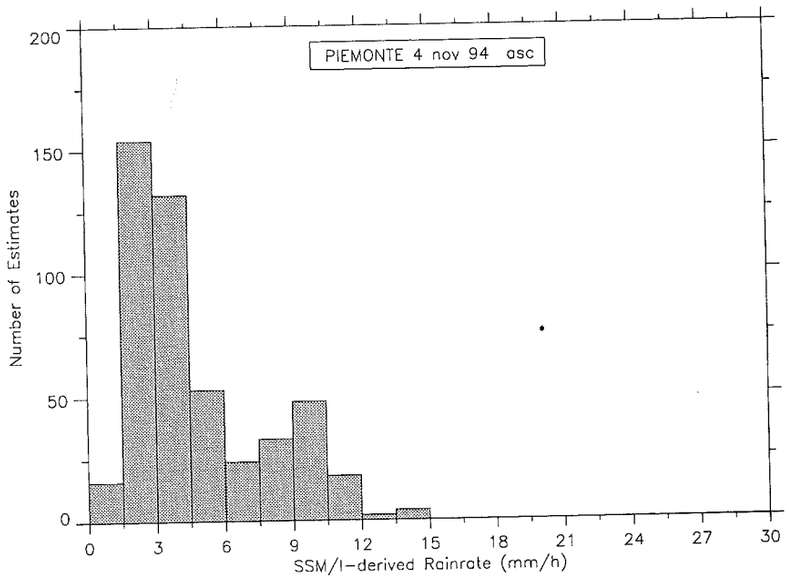

FIGURE 17 Rainfall rate histograms derived from SSM/I data for the precipitation areas over land of Figure 14.

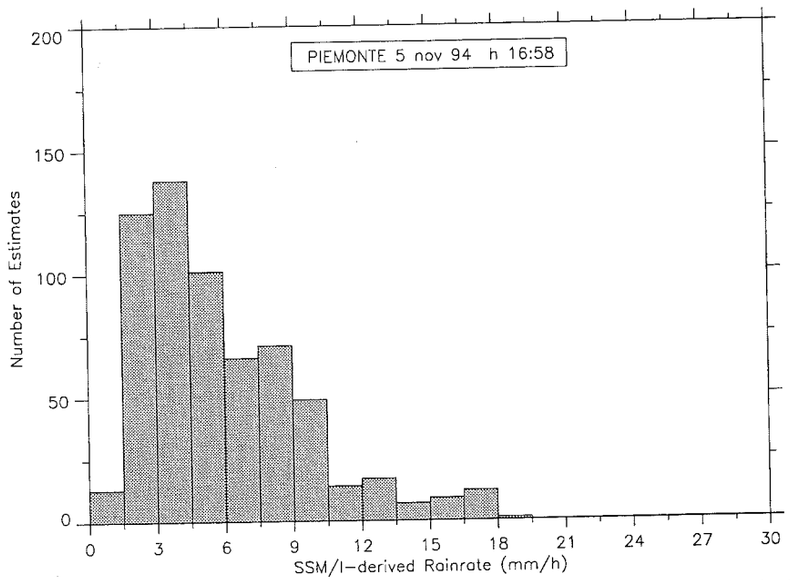

FIGURE 18 Rainfall rate histograms derived from SSM/I data for the precipitation areas over land of Figure 15.

should be used in the interpretation of data from satellite sensors, especially when the modeling, monitoring and forecasting of precipitation at smaller spatial scales than those of the sensor resolution are operationally involved.

Acknowledgments

The work presented in this paper was supported by the Commission of the European Communities, DG XII, Environment Programme, Climatology and Natural Hazard Unit, in the framework of the Contract No. EV5V-CT92-0167, "Flood Hazard Control by Multisensor Storm Tracking in the Mediterranean Area", code-named STORM'93 (Storm Tracking and Observation for Rainfall-Runoff Monitoring). The financial support of the European Space Agency (ESA) (ESA-ESTEC contract N.142042) and of an Italian National Research Council grant, under the framework of the National Group for Prevention from Hydrogeological Disasters (GNDCI) is also gratefully acknowledged. ESA is particularly acknowledged for the permission to use SAR images of the flooding event of November, 1994. SSM/I data have been provided by the NASA WetNet Project, directed by Dr. James Dodge.

References

Atlas, D. and Thiele, O.W. (1981): *Precipitation Measurements from Space*. Workshop Report DI54-8 NASA, Greenbelt MD.

Barrett E.C. and Martin, D.W. (1981): *The use of satellite data in rainfall monitoring*, Academic Press, London.

Barrett, E.C., and Beaumont, M.J. (1994): Satellite rainfall monitoring: An overview. *Remote Sensing Reviews*, **11(1–4)**, 23–48.

Basili, P., Ciotti, P., d'Auria, G., Marzano, F.S., Pierdicca, N. and Mugnai, A. (1992a): Cloud microphysical model application to multivariate analysis of satellite microwave radiometric data. *Specialists Meeting on Microwave Radiometry and Remote Sensing Applications*, Boulder, Colorado, USA, 14–16 January 1992, E.R. Westwater, (ed.), National Technical Information Service, Springfield, Virginia, USA, 245–249.

Basili, P., Ciotti, P., d'Auria, G., Marzano, F.S., Pierdicca, N. and Mugnai, A. (1992b): A simulation study for retrieving rainfall from space-borne microwave radiometers. *Specialists Meeting on Microwave Radiometry and Remote Sensing Applications*, Boulder, Colorado, USA, 14–16 January 1992, E.R. Westwater (ed.), National Technical Information Service, Springfield, Virginia, USA, 251–255.

Basili, P., Ciotti, P., d'Auria, G., Marzano, F.S., Pierdicca, N. and Mugnai, A. (1994): A statistical algorithm for retrieving precipitating cloud profile from spaceborne microwave radiometers, *Progress In Electromagnetics Research Symposium (PIERS) 1994*, pp. 453–456, Nordwijk (The Netherlands), 11–14 July.

Bolla, R., Boni, G., La Barbera, P., Lanza, L., Marchese, M. and Zappatore, S. (1995): The Tracking and Prediction of High Intensity Rainstorms. *Remote Sensing Reviews*. This Issue.

Boni, G., Lanza, L. and Conti, M. (1995): Assessing the role of cloud tracking through the analysis of animated sequences of satellite images. *Proceedings of XIV IASTED International Conference on Modeling, Identification and Control*, Innsbruck, Austria, February 20–23, 361–364.

Dodge, J. and Goodman, M. (1994): The WetNet Project. *Remote Sensing Reviews*, **11(1–6)**, 5, 21.

Farrar, M.R. and Smith, E.A. (1992): Spatial resolution enhancement of terrestrial features using deconvolved SSM/I microwave brightness temperatures. *IEEE Transactions of Geosciences and Remote Sensing*, **2**, 349–355.

French, M.N. and Krajewski, W.F. (1994): A model for real-time quantitative rainfall forecasting using remote sensing. 1. Formulation. *Water Resources Research*, **30**(4), 1075–1083.

Grody, N. (1991): Classification of snow cover and precipitation using the Special Sensor Microwave Imager. *Journal of Geophysical Research*, **96**, 7423–7435.

Hollinger, J.P., Pierce, J.L. and Poe, G.A. (1990): SSM/I instrument evaluation. *IEEE Transactions of Geosciences & Remote Sensing*, **GE-28**, Special Issue on the Defense Meteorological Satellite Program (DMSP): Calibration and Validation of the Special Sensor Microwave Imager (SSM/I), J.P. Hollinger (ed.), 781–790.

La Barbera, P. and Lanza, L. (1995): The use of remote sensing in rainfall monitoring and forecasting. *Excerpta*, **8**, 135–153.

Maddox, R.A. (1980): Mesoscale convective complexes. *Bulletin of the American Meteorological Soc.* **61**, 1374–1387.

Marzano, F.S., Mugnai, A., Smith, E.A., Xiang, X., Turk, J. and Vivekanandan, J. (1994): Active and passive remote sensing of precipitating storms during CaPE. Part II: Intercomparison of precipitation retrievals over land from AMPR radiometer and CP-2 radar. *Meteorology & Atmospheric Physics*, **54**, 24–59.

Marzano, F.S., Mugnai, A., Pierdicca, N., Smith, E.A., Turk, J. and Vivekanandan, J. (1995): Precipitation profile retrieval from airborne microwave radiometers: A case study over ocean during CaPE. *Specialist Meeting on Microwave Radiometry and Remote Sensing of the Environment*, Rome, Italy, 14–16 February 1994, D. Solimini, Ed., VSP, International Science Publ., Utrecht, The Netherlands, in press.

Mugnai, A., Cooper, H.J., Smith, E.A. and Tripoli, G.J. (1990): Simulation of microwave brightness temperatures of an evolving hailstorm at SSM/I frequencies. *Bulletin of the American Meteorological Society*, **71**, 2–13.

Mugnai, A., Smith, E.A. and Xiang, X. (1992): Passive microwave precipitation retrieval from space: A hybrid statistical-physical algorithm. *Specialists Meeting on Microwave Radiometry and Remote Sensing Applications*, Boulder, Colorado, USA, 14–16 January 1992, E.R. Westwater, Ed., National Technical Information Service, Springfield, Virginia, USA, 237–244.

Mugnai, A., Smith, E.A. and Tripoli, G.J. (1993): Foundations for statistical-physical precipitation retrieval from passive microwave satellite measurements. Part II: Emission source and generalized weighting function properties of a time-dependent cloud-radiation model. *Journal of Applied Meteorology*, **32**, 17–39.

Mugnai, A., Marzano, F.S. and Pierdicca, N. (1994): Precipitation profile retrieval from spaceborne multifrequency microwave radiometers: description and application of a maximum-likelihood algorithm. *Proceedings of CLIMPARA Symposium*, pp. 345–349, Moscow (Russia), 31 May–3 June 1994.

Ramis, C., Alonso, S. and Llasat, M.C. (1995): A comparative study between two cases of extreme rainfall events in Catalonia. *Surveys in Geophysics*, **16**(2): 141–161.

Smith, E.A., Mugnai, A., Cooper, H.J., Tripoli, G.J. and Xiang, X. (1992): Foundations for statistical-physical precipitation retrieval from passive microwave satellite measurements. Part I: Brightness-temperature properties of a time-dependent cloud-radiation model. *Journal of Applied Meteorology*, **31**, 506–531.

Smith, E.A., Kummerow, C. and Mugnai, A. (1994a): The emergence of inversion-type profile algorithms for estimation of precipitation from satellite passive microwave measurements. *Remote Sensing Reviews*, **11(1–4)**, 163–194.

Spencer, R.W., Goodman, H.M. and Hood, R.E. (1989): Precipitation retrieval over land and ocean with the SSM/I: Identification and characteristics of the scattering signal. *Journal of Atmospheric Oceanic & Technology*, **6**, 254–273.

Tripoli, G.J. (1992): A nonhydrostatic model designed to simulate scale interaction. *Monthly Weather Review*, **120**, 1342–1359.

Wilheit, T., Adler, R., Avery, S., Barrett, E.C., Bauer, P., Berg, W., Chang, A., Ferriday, J., Grody, N., Goodman, S., Kidd, C., Kniveton, D., Kummerow, C., Mugnai, A., Olson, W., Petty, G., Shibata, A., Smith, E.A. and Spencer, R.W. (1994): Algorithms for the retrieval of rainfall from passive microwave measurements. *Remote Sensing Review*, **11(1–4)**.

WMO (1989): *The Global Precipitation Climatology Project*, Report of the 4th Session of the International Working Group on Data Management, Bristol, U.K., 26–28 July 1989, WMO/TD 356. World Meteorological Organization, Geneva, Switzerland.